УДК 532.51

A Model of Averaged Molecular Viscosity for Turbulent Flow of Non-Newtonian Fluids

Andrey A. Gavrilov*
Institute of Physics, SB RAS,
Akademgorodok, 50/44, Krasnoyarsk, 660036
Russia

Valeriy Ya. Rudyak†
Novosibirsk State University of Architecture and Civil Engineering,
Leningradskaya, 113, Novosibirsk, 630008
Russia

Received 24.04.2013, received in revised form 09.10.2013, accepted 10.11.2013

A novel turbulence model for flows of viscoplastic fluid is presented. It is based on the Reynolds-Averaged approach. A closed model for the averaged viscosity that takes into account its nonlinear dependence on the fluctuating rate of deformation tensor is proposed. Test calculations were performed for power-law fluid and Herschel–Bulkley fluid flows in a straight round pipe. Numerical data obtained with the use of the proposed model are compared with the results of direct numerical simulations. The proposed model adequately describes the reduction in the turbulent transport of momentum with decreasing power-law index and with increasing yield stress of the fluid.

Keywords: shear-thinning fluids, Reynolds averaging, turbulent flow models, finite volume method.

Non-Newtonian fluid flows in pipes and annular channels are mostly turbulent and they are found in many applications. Despite this, experimental data on these flows are extremely scarce. The lack of systematic experimental data on turbulent flows of non-Newtonian fluids and their practical significance have motivated recent numerical simulations of such flows. In this way the central problem is the lack of closed well-founded and experimentally validated turbulence model for non-Newtonian fluids flow and, in particular, for viscoplastic fluids flow. In recent years, a number of studies have focused on the development of mathematical model for flows of power-law fluids [1, 2]. However, the model developed in these studies cannot be directly extended to yield-stress non-Newtonian fluids and it is only applicable to flows with relatively simple geometry. Thus, there is an urgent need for developing of numerical algorithms for simulations of non-Newtonian fluid flows on a regular basis. The present paper deals with the development of such an algorithm. The algorithm is based on the control volume approach developed previously by the authors to address a wide range of problems [3–5]. Power-law and Herschel–Bulkley fluids flows are considered. A two-parameter turbulence model and averaged effective molecular viscosity are used. Test calculations were performed for power-law and Herschel–Bulkley fluid flows in a straight round pipe. Numerical data obtained using the proposed model are compared with the results of direct numerical simulations [6, 7].

*gavand@yandex.ru
†valery.rudyak@mail.ru

1. Mathematical model

We consider isothermal steady flows of an incompressible non-Newtonian fluid. Such flows are described by the following hydrodynamic equations:

$$\nabla \cdot (\rho \mathbf{u}) = 0, \quad \rho \frac{\partial \mathbf{u}}{\partial t} + \nabla \cdot (\rho \mathbf{u}\mathbf{u}) = -\nabla p + \nabla \tau, \tag{1}$$

where ρ and $\mathbf{u}$ are the density and velocity of the fluid, p is the pressure and τ is the stress tensor. For the viscoplastic non-Newtonian fluids considered here, the stress tensor is proportional to the strain rate tensor $\mathbf{S}$:

$$\tau = 2\mu \mathbf{S}, \quad S_{ij} = \frac{1}{2}\left(\frac{\partial u_j}{\partial x_i} + \frac{\partial u_j}{\partial x_i}\right),$$

where the effective viscosity of the fluid depends on the shear rate $\dot{\gamma}$: $\mu = \mu(\dot{\gamma})$, $\dot{\gamma} = \sqrt{2\mathbf{S} \cdot \mathbf{S}}$. In what follows we consider fluids with a power law rheological model (power-law fluids) and Herschel–Bulkley fluids, for which the effective molecular viscosity is given by the formula:

$$\mu = \dot{\gamma}^{-1}\left(\tau_0 + k_\nu \dot{\gamma}^n\right), \tag{2}$$

where τ_0 is the yield point of the viscoplastic fluid, k_ν is the consistency and n is the flow index. For $\tau_0 = 0$, we obtain from (2) the effective viscosity of a power-law fluid and for $n = 1$ we obtain the effective viscosity of a Bingham fluid.

In what follows we consider fully developed turbulent flows of these fluids. To describe these fluids we will use the Reynolds averaging of basic equations of hydrodynamics (1) (RANS approach). Taking into account viscosity fluctuations, the RANS averaging of the continuity and momentum equations gives the following Reynolds equation:

$$\nabla \cdot \mathbf{U} = 0, \quad \rho \mathbf{U} \cdot \nabla \mathbf{U} = -\nabla P + \nabla \cdot (2\mu \mathbf{S}) + \nabla \cdot \left(-\rho \left\langle \mathbf{u}'\mathbf{u}' \right\rangle\right) + \nabla \cdot \left\langle 2\mu' \mathbf{S}' \right\rangle \tag{3}$$

Here $\mathbf{U}$ is the averaged fluid velocity, P is the averaged pressure, $\mathbf{S}$ is the averaged strain rate tensor and μ is the averaged molecular viscosity. The angle brackets denote averaging over time and the prime refers to the fluctuating quantities. The additional term in the right-hand side of equation (3) is introduced for non-Newtonian fluids since in this case the molecular viscosity depends not only on the mean flow velocity but also on the fluctuations of the velocity field.

In what follows we use the two-parameter k-ε turbulence model [1, 2]. In the context of this model the system of Reynolds equations (3) is supplemented by transport equation for the mean turbulence energy k and by equation for the mean rate of its dissipation ε :

$$\rho U_i \frac{\partial k}{\partial x_i} = \frac{\partial}{\partial x_i}\left(\left(\mu + \frac{\mu_t}{\sigma_k}\right)\frac{\partial k}{\partial x_i}\right) + P_k - \rho\varepsilon - 2\left\langle \mu' S'_{ij} \right\rangle S_{ij}, \tag{4}$$

$$\rho U_i \frac{\partial \varepsilon}{\partial x_i} = \frac{\partial}{\partial x_i}\left(\left(\mu + \frac{\mu_t}{\sigma_\varepsilon}\right)\frac{\partial \varepsilon}{\partial x_i}\right) + C_1 \frac{\varepsilon}{k} P_k - C_2 \rho \frac{\varepsilon^2}{k} + \left\langle u_k \frac{\partial \hat{\mu}}{\partial x_k}\left(2 S'_{ij} S'_{ij}\right)\right\rangle, \tag{5}$$

where turbulence generation is given by expression $P_k = \tau^t \cdot \nabla \mathbf{U}$; the cap ($\hat{\mu}$) refers to instantaneous values. In the case of non-Newtonian fluids the standard k-ε model is modified by introducing additional terms into transport equations (4)–(5).

Reynolds stress is modeled using the Boussinesq hypothesis:

$$\tau^t_{ij} = -\rho \left\langle u'_i u'_j \right\rangle = \mu_t \left(\frac{\partial U_j}{\partial x_i} + \frac{\partial U_j}{\partial x_i}\right) - \rho \frac{2}{3}\delta_{ik} k, \tag{6}$$

where μ_t is the turbulent viscosity.

To close equations (3)–(6) it is necessary to have expressions for the last two correlation terms on the right-hand side of transport equations (4) and (5) and an expression for the mean molecular viscosity. The effective molecular viscosity of a fluid depends not only on the mean flow velocity but also on the fluctuations of the velocity field. To take this into account we represent the instantaneous local value of the molecular viscosity $\hat{\mu}$ as the sum of the mean μ and fluctuating μ' values: $\hat{\mu} = \mu + \mu'$. The instantaneous rate of dissipation of turbulent energy $\hat{\varepsilon}$ which characterizes the mean energy converted to heat in unit fluid mass per unit time is given by $\rho\hat{\varepsilon} = \hat{\mu}\hat{\dot{\gamma}}^2$. We further assume that the mean value is given by the relation of the same structure:

$$\rho\varepsilon = \mu \left\langle 2S'_{ij}S'_{ij} \right\rangle. \tag{7}$$

Here we omit the correlations between molecular viscosity fluctuations and shear rate fluctuations. The mean shear rate is expressed as the sum of two terms:

$$\dot{\gamma}^2 = 2\left\langle \hat{S}_{ij}\hat{S}_{ij} \right\rangle = 2S_{ij}S_{ij} + \left\langle 2S'_{ij}S'_{ij} \right\rangle.$$

The first term on the right-hand side is calculated from the gradients of the mean velocity and the second term defines the mean fluctuating shear rate. Using relation (7), for the mean shear rate we obtain:

$$\dot{\gamma}^2 = 2S_{ij}S_{ij} + (\rho\varepsilon)/\mu. \tag{8}$$

Using the same approximation, we can assume that the mean molecular viscosity is again related to the mean shear rate by formula (2).

Thus, the mean molecular viscosity can be found by solving the system of nonlinear equations (2) and (8). Because solving the Reynolds equations closed by the chosen turbulence model involves some iterative process there is no need to have an exact algebraic expression or an approximate numerical expression for the dependence of the viscosity on the dissipation rate and on the mean strain rate tensor. To find the distribution of the mean molecular viscosity the following two-step iterative algorithm is proposed. In the first step the local mean shear rate is calculated from the current values of the mean velocity, dissipation rate and molecular viscosity by formula (8). Then, the obtained mean shear rate is used to determine the mean effective molecular viscosity from equation (2). The obtained viscosity is then used to solve the hydrodynamic equations on the next iteration step.

Near-wall turbulent flows are characterized by the substantial dissipation of turbulence near the wall, even in the viscous sublayer. Therefore, to calculate the mean viscosity at the wall it is necessary to take into account the terms related to small-scale shear. The molecular viscosity at the wall is calculated by the iterative algorithm given above which is used in the control volumes of the computational domain. The tangential stress at the wall is calculated from the obtained viscosity near the wall and the normal gradient of the mean velocity component tangential to the wall: $\tau_w = \mu_w(\partial U/\partial n)_w$.

Since we neglected the correlation between the viscosity and the strain rate tensor in the construction of the averaged-viscosity model it is reasonable to drop the corresponding terms in the transport equation for the momentum (3) and in the transport equation for turbulence energy (4). Finally, the system of differential equations has the form:

$$\frac{\partial U_i}{\partial x_i} = 0, \quad \rho U_k \frac{\partial U_i}{\partial x_k} = -\frac{\partial P}{\partial x_i} + \frac{\partial}{\partial x_k}\left(\left(\mu + \mu_t\right) 2S_{ij}\right) - \rho\frac{2}{3}\frac{\partial k}{\partial x_i}. \tag{9}$$

These equations are closed by the transport equation for the turbulent energy

$$\rho U_i \frac{\partial k}{\partial x_i} = \frac{\partial}{\partial x_i}\left(\left(\mu + \frac{\mu_t}{\sigma_k}\right)\frac{\partial k}{\partial x_i}\right) + P_k - \rho\varepsilon, \tag{10}$$

and by the transport equation for the turbulent energy dissipation rate

$$\rho U_i \frac{\partial \varepsilon}{\partial x_i} = \frac{\partial}{\partial x_i}\left[\left(\mu + \frac{\mu_t}{\sigma_\varepsilon}\right)\frac{\partial \varepsilon}{\partial x_i}\right] + C_{\varepsilon 1}\frac{\varepsilon}{k}P_k - C_{\varepsilon 2}\rho\frac{\varepsilon^2}{k}. \tag{11}$$

The turbulent viscosity is given by the algebraic relation: $\mu_t = \rho c_\mu f_\mu k^2/\varepsilon$, where c_μ is a constant and f_μ is a damping function which will be described below.

There are many low Reynolds number k–ε models for Newtonian fluids. Those models differ by the form of the extra terms and damping functions. For the purposes of this paper the choice of specific turbulence model is not important. Further, in the construction of a particular numerical algorithm, the low-Reynolds k–ε model of Abe et al. [8] is used. This model is a modification of the two-parameter dissipative k–ε turbulence model for near-wall flows. Two special damping factors are introduced to adequately describe the behavior of turbulent parameters in the immediate vicinity of the wall and to take into account the damping effect of the wall on turbulence. The first factor is included in the expression for the turbulent viscosity: $\mu_t = \rho c_\mu f_\mu k^2/\varepsilon$, where

$$f_\mu = \left[1 - \exp\left(-\frac{Re_\varepsilon}{14}\right)\right]^2 \left[1 + \frac{5}{Re_t^{3/4}} \cdot \exp\left\{-\left(\frac{Re_t}{200}\right)^2\right\}\right],$$

and the second factor is included in the transport equation for the dissipation rate $C^*_{\varepsilon 2} = C_{\varepsilon 2} f_2$

$$f_2 = \left[1 - \exp\left(-\frac{Re_\varepsilon}{3.1}\right)\right]^2 \left[1 - 0.3 \cdot \exp\left\{-\left(\frac{Re_t}{6.5}\right)^2\right\}\right].$$

Here the turbulent Reynolds number and the dimensionless distance to the wall are

$$Re_t = \frac{k^2}{\varepsilon\nu}, Re_\varepsilon = \frac{(\varepsilon\nu)^{1/4} y}{\nu},$$

where y is the distance to the wall and ν is the kinematic viscosity. The constants in these expressions have the following values [8]: c_μ= 0.09, σ_k= 1.4, σ_ϵ= 1.4, $C_{\epsilon 1}$= 1.5 and $C_{\epsilon 2}$= 1.9. The model was chosen for its good performance in the case of Newtonian fluid flow in a pipe. In the present formulation, the two-parameter k–ε turbulence model is modified only by including the dependence of the mean molecular viscosity on the mean and fluctuating flow parameters. The damping functions and model parameters have not been changed and we assume the forms and the numerical values used in Newtonian fluid mechanics.

2. Numerical algorithm

The model discussed above has been implemented in in-house CFD code σFlow. Details of its implementation for laminar Newtonian fluids flows are described in our paper [9]. The code employs the finite-volume discretization method. In the finite volume method, computational domain is divided into a number of control volumes (or cells). All dependent variables are stored at the geometric center of the control volume, i.e. they are co-located. The finite-volume method is based on integration of the differential form of the governing equations over each control volume. In the process of discretization both surface and volume integrals are approximated with the use of the mid-point rule. The convective terms of the transport equations are approximated using a second-order upwind UMIST TVD scheme [10]. The diffusive fluxes are discretized using the central difference scheme with second-order accuracy. On collocated grids, a special interpolation procedure is required for the face velocities. Oscillations of the pressure field are eliminated using the Rhie–Chow approach which involves a special interpolation of the velocity at the faces of the control volumes.

The overall solution procedure is iterative and it is based on the SIMPLEC segregated algorithm [11]. The procedure employs a predictor-corrector strategy. The flow equations are temporarily decoupled from each other so that they can be solved sequentially. The algorithm effectively couples the velocity and pressure fields by converting the discrete form of the continuity equation into equation for the pressure correction. In order to improve convergence the procedure of under-relaxation is applied to all transport equations in an implicit manner. The implicit form of under-relaxation consists in addition of an artificial diagonal term to the left hand side of equation. The values of under relaxation factors for every transport equation were set to 0.8.

The linearized algebraic equations for transport equations are solved by preconditioned conjugate residuals methods [12]. The system of algebraic equations obtained after discretization of the pressure correction equation is solved by the algebraic multigrid solver [13].

The main stages of the algorithm at each iteration step l are summarized:

1. The approximate velocity field is obtained by solving the momentum equation (9):

$$\frac{\rho(U^* - U^{l-1})}{\tau} = -\nabla \cdot \left(\rho U^{l-1} U^*\right) + \nabla \cdot \left[2\left(\mu^{l-1} + \mu_t^{l-1}\right) S^*\right] - \rho\frac{2}{3}\nabla k^{l-1} - \nabla p^{l-1}$$

$$\tau = \frac{\rho Vol_P}{a_P}\frac{\alpha}{1-\alpha}$$

where τ is a pseudo time step introducing by under-relaxation, Vol_P is the control cell volume, a_P is the center coefficient of the discretized convective and diffusive terms of momentum equations and α is the under-relaxation factor. The pressure gradient term is calculated using the pressure distribution from the previous iteration.

2. The elliptic equation for pressure correction $\delta p = p^l - p^{l-1}$ is solved in order to obtain the new pressure distribution: $\nabla \cdot (\tau \nabla \delta p) = \nabla \cdot (\rho U^*)$.

3. The explicit velocity correction is performed using pressure correction gradient so that the velocity components satisfy the continuity equation:

$$\delta U = -\frac{\tau}{\rho}\nabla(\delta p), \quad U^l = U^* + \delta U.$$

4. The discretized transport equation for turbulent energy (10) and transport equation for dissipation rate (11) are solved using the available velocity fields and averaged molecular viscosity. Then the turbulent viscosity is updated.

5. The local mean shear rate is calculated using the averaged molecular viscosity from previous iteration: $\dot{\gamma}^2 = 2S_{ij}^l S_{ij}^l + \rho\varepsilon^l/\mu^{l-1}$. Then, obtained mean shear rate is used to calculate the averaged molecular viscosity on a new iteration layer: $\mu^l = \dot{\gamma}^{-1}(\tau_0 + k_\nu \dot{\gamma}^n)$.

6. The following convergence criterion for momentum equation is used:

$$\left\|U^l - U^{l-1}\right\| / \left\|U^l\right\| < \delta,$$

where δ is equal to 10^{-8}. If this criterion is not fulfilled, a new iteration starts.

All equations are integrated to the wall. The wall treatment assumes that the viscous sublayer is well resolved and requires the first computational cell above the wall to be located within the viscous sublayer. Hence fine grids are needed for the wall treatment because strong gradients of the flow and turbulence variables exist in the viscous layer. The coordinate of the first cell $y^+ \sim 0.5$, where $y^+ = \rho y u_\tau/\mu_w$ is dimensionless distance to the wall normalized by the friction velocity $u_\tau = \sqrt{\tau_w/\rho}$ and by the averaged molecular viscosity at the wall μ_w.

The no-slip condition for velocity and Dirichlet boundary condition for turbulent kinetic energy $k_w = 0$ are used at walls. The exact wall-limiting value of ε can be deduced from the turbulence energy budget. At the near-wall cell the turbulent dissipation rate is specified according to the formula $\varepsilon = \nu 2k/y^2$, where y is the normal distance from the wall.

The main difficulty in modeling viscoplastic flows, including turbulent regimes, is associated with the existence of singular molecular viscosity in the regions where the shear rate is zero. This difficulty is overcome by using various regularizations of the basic rheological models. In algorithm developed here an approximation proposed by Papanastasiou [14] is used. The effective viscosity is approximated by some smooth function. For Herschel–Bulkley fluids, the expression $\mu = (\tau_0 + k_\nu \dot{\gamma}^n)\dot{\gamma}^{-1}$ is replaced by

$$\mu = [k_\nu \dot{\gamma}^n + \tau_0 \left(1 - \exp(-m\dot{\gamma}/\Gamma)\right] \dot{\gamma}^{-1},$$

which limits the effective viscosity as the shear rate tends to zero. Here Γ is a characteristic shear rate and m is a regularization parameter. The dimensionless parameter m should be large enough (its value varies from 100 to 3000 in most papers).

3. Results and Discussion

This section presents test calculations of steady turbulent flow in a straight round pipe for power-law fluids and Herschel–Bulkley fluids for various power-law indices and yield stresses.

3.1. Power law fluids

The calculations were performed for regimes studied by direct numerical simulation (DNS). The calculations for power-law fluids were made for the three regimes studied using DNS in [6]. The generalized Reynolds number $Re_w = (\rho U D)/\mu_w$ of the investigated regimes was about 5500 (here μ_w is the mean effective viscosity at the wall, U is the mean flow velocity and D is the diameter of the channel). The generalized Reynolds number accounts for the flow behavior in the vicinity of the wall. It determines the formation and development of turbulence in near-wall flows. Thus the Reynolds number can be taken to be a measure for comparison of fluid flows with different rheological models.

The power-law index of the studied fluids and the generalized Reynolds number are given in the first two columns of Tab. 1. The next column gives the values of the Metzner–Reed Reynolds number numbers commonly used for non-Newtonian fluids [15]

$$Re_{MR} = \frac{4n\rho U^{2-n} D^n}{8^{n-1} k_\nu (3n+1)}.$$

The last two columns give the values of the drag coefficient $c = \tau_w/(\rho U^2/2)$ obtained with the use of the well-known Dodge–Metzner correlation c_{DM} [16] and calculated using the algorithm proposed in this paper.

Table 1. Non-dimensional parameters for the pipe flow simulations of power law fluids

n	Re_w	Re_{MR}	$c_{DM}, 10^{-3}$	$c, 10^{-3}$
0.75	5500	3968	8.48	8.38
0.69	5500	3700	8.24	8.04
0.5	5500	3126	7.21	6.52

Comparison of the calculated drag coefficients with the Dodge and Metzner correlation [16] shows that for large power-law indices of fluids they are in close agreement. The agreement becomes worse with decreasing index n. For example, for $n = 0.5$ the calculated value of drag coefficient is almost 10% lower than the value given by the correlation.

Normalized average axial velocity, Reynolds shear stresses and average molecular viscosity are shown in Fig. 1. The dependence of dimensionless velocity $U^+ = U/u_\tau$ on dimensionless

distance y^+ for the power-law fluids presented in Tab. 1 are shown in Figs. 1.1 and 1.2. Both the DNS and our calculations show the deviation of the velocity profile from the Newtonian profile with decreasing power-law index n. When index n decreases in the logarithmic sublayer ($y^+ > 30$) the average velocity profile lies above the Newtonian profile and the slope of the profile increases. In the laminar and buffer sublayers ($y^+ < 10$) the calculated profiles are similar and they are almost linearly dependent on the distance as for Newtonian flows with constant viscosity. Our calculated average velocity profiles lie slightly above the DNS data. It means that the drag coefficient is underestimated. The average velocity profile for $n = 0.5$ obtained in [6] lies well above the other profiles. Rudman et al. [6] explain this by the fact that the flow with $n = 0.5$ is a transitional flow with not fully developed turbulent core.

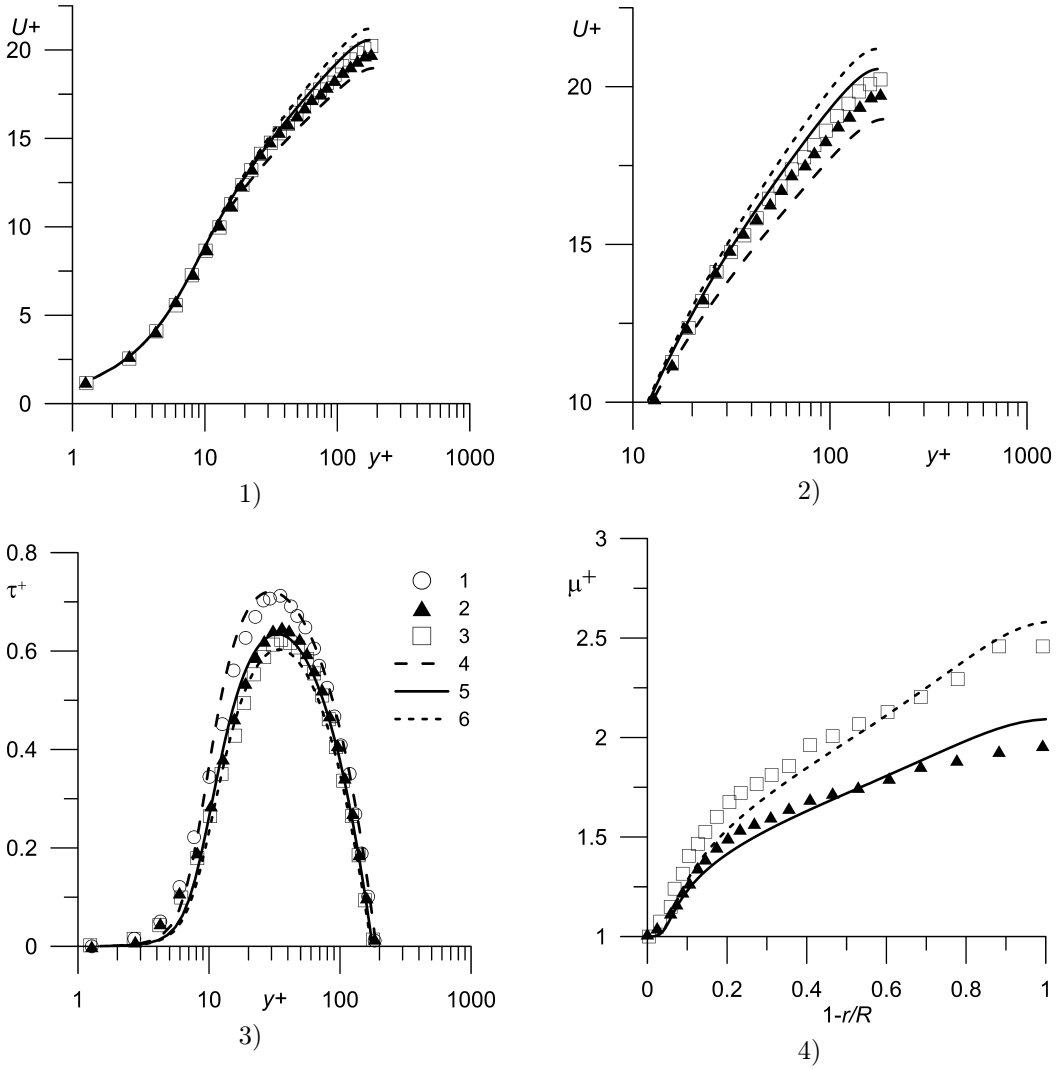

Fig. 1. Average flow profiles for power law fluid: 1–2) axial velocity; 3) Reynolds shear stress; 4) normalized averaged molecular viscosities along the pipe radius. Symbols correspond to DNS (1 — n=1, 2 — n=0.75, 3 — n=0.69) and lines correspond to RANS (4 — n=1, 5 — n=0.75, 6 — n=0.69)

The dependence of the dimensionless turbulent shear stress $\tau_t = -\mu_t(\partial U/\partial y)$ on dimensionless distance are shown in Fig. 1.3. The shear stress is calculated from the average velocity profile

and turbulent viscosity. The symbols correspond to the data presented in [6]. In all cases the DNS data are in close agreement with our calculations. When index n decreases, the maximum of the profile of turbulent fluctuations decreases and its position is slightly shifted from the wall. This change in the Reynolds stress profile with decreasing index n is due to increase in molecular viscosity in the flow core. The increase in molecular viscosity results in weakening of the turbulent transport of momentum from the flow core to the wall.

Finally, Fig. 1.4 shows the distributions of the normalized average molecular viscosity $\mu^+ = \mu/\mu_w$ obtained using the proposed RANS model and DNS. In all cases there is good agreement between these data over the entire flow region. Our results and DNS results show monotonic increase in the average molecular viscosity with distance from the wall. The ratio of the viscosity in the flow core to the viscosity at the wall increases when index n decreases; for $n = 0.75$ this ratio is close to 2 and for $n = 0.69$ the ratio is about 2.5.

If velocity fluctuations are ignored then the average viscosity is significantly overestimated. Fig. 2 shows predicted radial profiles of normalized average molecular viscosity in comparison with the model of Cruz and Pinho [2] for power law fluids. Whereas our model can adequately predict the behavior of the average viscosity, the model of Cruz and Pinho overestimates the viscosity value in comparison with DNS data. The gross overestimation of the viscosity is observed over the entire flow region with the exception of viscous sublayer. This discrepancy is produced by modification of damping function which takes into account fluids with different rheological models. With large damping the molecular viscosity remains basically unaffected by turbulence and it is described by the expression for laminar flow except for the central region of the pipe. One should also note that the model of Cruz and Pinho cannot be directly extended to yield-stress non-Newtonian fluids.

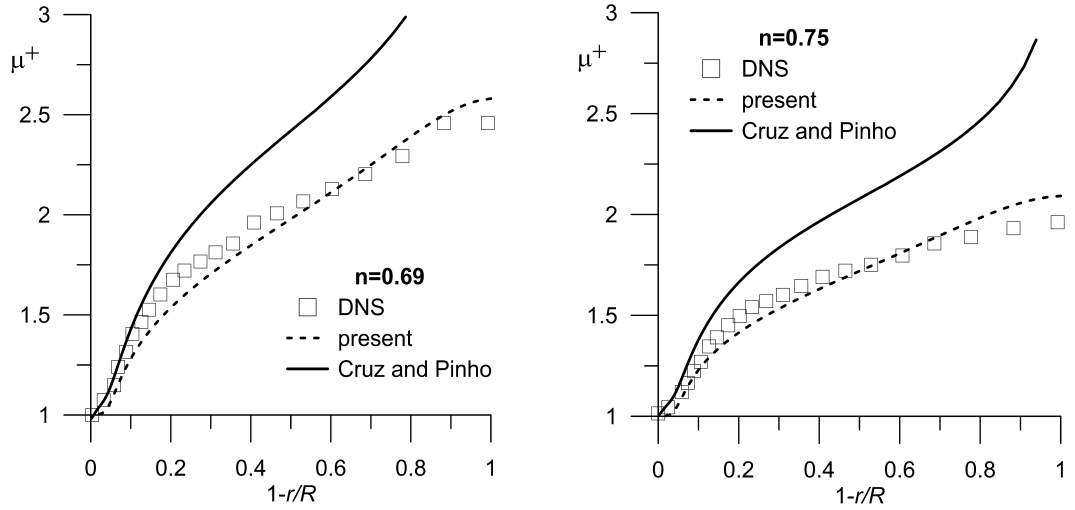

Fig. 2. Normalized average molecular viscosities along the pipe radius for power-law fluids

3.2. Herschel–Bulkley fluids

The second series of calculations was performed for the flow regimes and fluids studied by DNS in [7]. The necessary data are given in Tab. 2. The following notations are introduced in the table: NF — Newtonian fluid, PL — power law fluid and HB — Herschel–Bulkley fluid. The table also gives the values of the friction coefficient at the wall. The values of the drag coefficient obtained in [7] are listed in the next to last column. The values of the drag coefficient obtained in our study are listed in the last column.

Table 2. Non-dimensional parameters for the pipe flow simulations of Herschel–Bulkley fluids

case	n	τ_0/τ_w	Re_w	$c_{DNS}, 10^{-3}$	$c, 10^{-3}$
NF	1.0	0.0	7400	8.64	8.7
PL	0.6	0.0	7300	7.43	6.97
HB	0.6	0.1	7200	6.84	6.29

Normalized average axial velocity, Reynolds shear stresses, turbulent kinetic energy and average molecular viscosity are shown in Fig. 3. The velocity profiles obtained in this case are presented in Fig. 3.1. Here the symbols correspond to the DNS data [7] and various curves correspond to our data. As in the previous case, the velocity profiles in the logarithmic sublayer

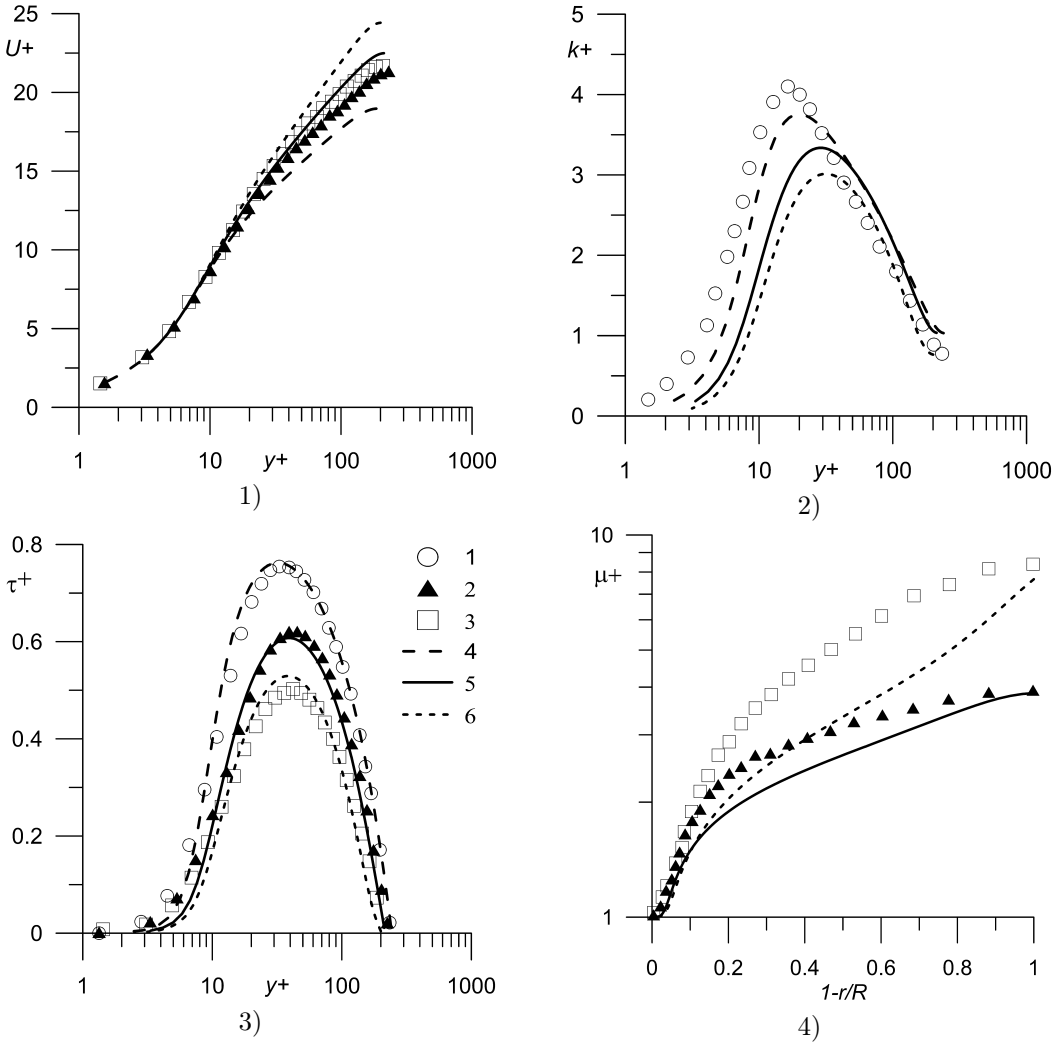

Fig. 3. Mean flow profiles: 1) axial velocity; 2) turbulent energy; 3) Reynolds shear stress; 4) normalized molecular viscosities along the pipe radius. Symbols correspond to DNS (1 — NF; 2 — PL, 3 — HB), and lines to RANS (4 — NF, 5 — PL, 6 — HB)

are above the profile characteristic for Newtonian fluid. In this region, the slope of the calculated profile for Herschel–Bulkley fluids exceeds the slope of the DNS profile. This explains the distinction in the drag coefficient (see Tab. 2).

Turbulent stress distributions are presented in Figs. 3.2 and 3.3. One should note that in the DNS simulation the turbulent kinetic energy distributions for the regimes presented here slightly diverge from the Newtonian distribution and they are not shown in the figure. In our calculations for the non-Newtonian regimes the maximum of turbulent energy is significantly reduced (by almost 25% for Herschel–Bulkley fluids) and its position is shifted away from the wall toward the core of the flow (Fig. 3.2). For all regimes the distribution of turbulent shear stresses is close to DNS result (Fig. 3.3). As the yield stress increases, there is a significant decrease in the rate of turbulent transport of momentum which is reflected in the distribution. For Herschel–Bulkley fluid flow the stress peak decreases by 40% compared to Newtonian fluids. The position of the maximum is slightly shifted away from the wall.

The reduction in the turbulent exchange of momentum is apparently due to considerable increase in the molecular viscosity with distance from the wall. Comparison of the averaged viscosity distributions is given in Fig. 3.4. The distributions are normalized to the viscosity at the wall. All data show a monotonic increase in viscosity with distance from the wall. In the region $0 < y^+ < 10$ the average viscosity varies only slightly. In the region of maximum turbulence generation ($y^+ > 10$) there is a sharp increase in the average viscosity. RANS calculations give good prediction of the maximum magnitude of the average viscosity. For Herschel–Bulkley fluid flow the agreement with DNS data in the logarithmic sublayer is somewhat worse than that for power-law fluids.

Conclusions

The turbulent flow model presented in this paper makes it possible, for the first time, to simulate not only power-law fluids but also yield-stress fluids, in particular, Herschel–Bulkley fluids. Despite the correlations omitted in the construction of the averaged-viscosity model, the presented model provides a good prediction of the averaged-viscosity distributions in the boundary layer and in the flow core. Within the framework of the RANS approach the proposed model adequately describes the reduction in the turbulent transport of momentum with decreasing power-law index of the fluid.

At the same time, this model can be further improved. First, the turbulence model employed can be modified to describe non-Newtonian fluid flows. The absence of such a modification leads to large discrepancies with the DNS data for flows of fluids with rheological properties other than those characterizing Newtonian fluid (fluid with small indices n or/and with high yield stress). In particular, in the present study this makes itself evident in the stronger dependence of the velocity distributions on fluid rheological property (the index n) than it is predicted by DNS data.

Second, the DNS data suggest a higher anisotropy of turbulent fluctuations of non-Newtonian flow in comparison with Newtonian flows. The RANS model based on the eddy viscosity concept is inappropriate for describing flows with strong anisotropy of turbulent stresses. Our calculations showed that decreasing the fluid power-law-index n significantly diminishes the energy of turbulent fluctuations. This is not consistent with experiments and DNS calculations. Alternatively, the k–ε based turbulence model proposed by Durbin can be used. That model includes two additional equations to represent the near-wall turbulence anisotropy [17].

Finally, it should be noted that there are no references to DNS data regarding distributions for correlations of the form $\left\langle \mu' S'_{ij} \right\rangle$. Such data are necessary for the closure of the model. Therefore, it is necessary to perform a direct numerical simulation of turbulent flows with low Reynolds numbers in order to construct a more accurate model.

References

[1] F.T.Pinho, A GNF framework for turbulent flow models of drag reducing fluids and proposal for a k-e type closure, *Journal of Non-Newtonian Fluid Mechanics*, **114**(2003), 149–184.

[2] D.O.A.Cruz, F.T.Pinho, Turbulent pipe flow predictions with a low Reynolds number k-e model for drag reducing fluids, *Journal of Non-Newtonian Fluid Mechanics*, **114**(2003), 109–148.

[3] V.Ya.Rudyak, A.V.Minakov, A.A.Gavrilov, A.A.Dekterev, Application of new numerical algorithm for solving the Navier–Stokes equations for modelling the work of a viscometer of the physical pendulum type, *Thermophysics and Aeromechanics*, **15**(2008), no. 2, 333–345.

[4] V.Ya.Rudyak, A.V.Minakov, A.A.Gavrilov, A.A.Dekterev, Modelling of flows in micromixers, *Thermophysics and Aeromechanics*, **17**(2010), no. 4, 565–576.

[5] E.V.Podryabinkin, V.Ya.Rudyak, Moment and forces exerted on the inner cylinder in eccentric annual flow, *J. Engineering Thermophysics*, **20**(2011), no. 3, 320–328.

[6] M.Rudman, H.M.Blackburn, L.J.W.Graham, L.Pullum, Turbulent pipe flow of shear-thinning fluids, *J. Non-Newtonian Fluid Mech*, **118**(2004), 33–48.

[7] M. Rudman, H.M. Blackburn, Direct numerical simulation of turbulent non-Newtonian flow using a spectral element method, *Applied Mathematical Modelling*, **30**(2006), 1229–1248.

[8] K.Abe, T.Kondoh, Y.Nagano, A new turbulence model for predicting fluid flow and heat transfer in separating and reattaching flows–I. Flow field calculations , *Int. J. Heat Mass Transfer*, **37**(1994), no. 1, 139–151.

[9] A.A.Gavrilov, A.V.Minakov, A.A.Dekterev, V Ya.Rudyak, A numerical algorithm for modeling laminar flows in an annular channel with eccentricity , *Journal of Applied and Industrial Mathematics*, **5**(2011), no. 4, 559–568.

[10] F.S.Lien, M.A.Leschziner, Upstream monotonic interpolation for scalar transport with application to complex turbulent flows, *International Journal for Numerical Methods in Fluids*, **19**(1994), no. 6, 527-548.

[11] J.P.Van Doormal, G.D.Raithby, Enhancements of the SIMPLE Method for Predicting Incompressible Fluid Flows, *Numerical Heat Transfer*, **7**(1984), no. 2, 147–163.

[12] Y.Saad, Iterative methods for sparse linear systems, SIAM, 2000.

[13] U.Trottenberg, C.W.Oosterlee, A.Schuller, Multigrid, Academic Press, 2000.

[14] T.C.Papanastasiou, Flow of materials with yield, *Journal of Rheology*, **31**(1987), 385–404.

[15] A.B.Metzner, J.C.Reed, Flow of Non-Newtonian Fluids-Correlation of the Laminar, Transition, and Turbulent-Flow Regions, *Aiche Journal*, **1**(1955), 434–440.

[16] D.W.Dodge, A.B.Metzner, Turbulent flow of non-Newtonian system,*A.I.Ch.E. Journal*, **5**(1959), no. 2, 189–204.

[17] G.Iaccarino, E.S.G.Shaqfeha, Y.Dubief, Reynolds-averaged modeling of polymer drag reduction in turbulent flows, *Journal of Non-Newtonian Fluid Mechanics*, **165**(2010), no. 7–8, 376–384.

Модель осредненной молекулярной вязкости для турбулентных течений неньютоновских жидкостей

Андрей А. Гаврилов
Валерий Я. Рудяк

В статье представлена модель турбулентности для вязкопластических жидкостей. С использованием процедуры осреднения по Рейнольдсу разработана модель осредненной молекулярной вязкости для неньютоновских сред, учитывающая нелинейную зависимость от флуктуирующего тензора скоростей деформации. В качестве базовой модели турбулентности использована двухпараметрическая дифференциальная модель турбулентности. Тестовые расчеты выполнены для течений степенной жидкости и жидкости Гершеля–Балкли в прямой круглой трубе. Полученные расчетные данные сопоставлялись с результатами прямого численного моделирования. Предложенная модель позволяет правильно описать снижение турбулентного переноса импульса с уменьшением степени среды и с увеличением предельного напряжения.

Ключевые слова: вязкопластические жидкости, осреднение по Рейнольдсу, модель турбулентности, метод конечного объема.